available at www.sciencedirect.com

ScienceDirect

journal homepage: www.elsevier.com/locate/biochempharm

The membrane permeable calcium chelator BAPTA-AM directly blocks human ether a-go-go-related gene potassium channels stably expressed in HEK 293 cells

Qiang Tang [a,c], Man-Wen Jin [c], Ji-Zhou Xiang [c], Min-Qing Dong [a], Hai-Ying Sun [a], Chu-Pak Lau [a], Gui-Rong Li [a,b,*]

[a] Department of Medicine, Li Ka Shing Faculty of Medicine, The University of Hong Kong, Pokfulam, Hong Kong, SAR, China
[b] Department of Physiology, Li Ka Shing Faculty of Medicine, The University of Hong Kong, Pokfulam, Hong Kong, SAR China
[c] Department of Pharmacology, Tongji Medical College, Huazhang University of Science and Technology, Wuhan, Hubei, China

ARTICLE INFO

Article history:
Received 3 June 2007
Accepted 30 July 2007

Keywords:
BAPTA-AM
hERG
hKv1.3
hKv1.5
Open channel blocker

ABSTRACT

BAPTA-AM is a well-known membrane permeable Ca^{2+} chelator. The present study found that BAPTA-AM rapidly and reversibly suppressed human ether a-go-go-related gene (hERG or Kv11.1) K^+ current, human Kv1.3 and human Kv1.5 channel currents stably expressed in HEK 293 cells, and the effects were not related to Ca^{2+} chelation. The externally applied BAPTA-AM inhibited hERG channels in a concentration-dependent manner (IC_{50}: 1.3 μM). Blockade of hERG channels was dependent on channel opening, and tonic block was minimal. Steady-state activation $V_{0.5}$ of hERG channels was negatively shifted by 8.5 mV (from -3.7 ± 2.8 of control to -12.2 ± 3.1 mV, $P < 0.01$), while inactivation $V_{0.5}$ was negatively shifted by 6.1 mV (from -37.9 ± 2.0 mV of control to -44.0 ± 1.6 mV, $P < 0.05$) with application of 3 μM BAPTA-AM. The S6 mutant Y652A and the pore helix mutant S631A significantly attenuated blockade by BAPTA-AM at 10 μM causing profound blockade of wild-type hERG channels. In addition, BAPTA-AM inhibited hKv1.3 and hKv1.5 channels in a concentration-dependent manner (IC_{50}: 1.45 and 1.23 μM, respectively), and the blockade of these two types of channels was also dependent on channel opening. Moreover, EGTA-AM was found to be an open channel blocker of hERG, hKv1.3, hKv1.5 channels, though its efficacy is weaker than that of BAPTA-AM. These results indicate that the membrane permeable Ca^{2+} chelator BAPTA-AM (also EGTA-AM) exerts an open channel blocking effect on hERG, hKv1.3 and hKv1.5 channels.

1. Introduction

The membrane-permeable Ca^{2+} chelator BAPTA-AM (1,2-bis-(o-aminophenoxy)-ethane-*N*,*N*,*N*′,*N*′-tetraacetic acid, tetraacetoxymethyl esteris) developed by Tsien [1] contains four esters groups attached to the Ca^{2+} binding sites which confer its membrane permeability. By entering the cells, the esters are hydrolyzed by cytoplasmic esterases and the active compound BAPTA is revealed to act as an intracellular Ca^{2+} buffer [1]. BAPTA-AM has been widely used as an intracellular Ca^{2+} sponge to control the internal Ca^{2+} concentration in the studies on intracellular Ca^{2+} signals regulation of cellular physiological and biological functions [2,3] including ion channel activity [4–8].

* *Corresponding author at*: L8-01, Laboratory Block, Faculty of Medicine Building, The University of Hong Kong, 21 Sassoon Road, Pokfulam, Hong Kong, SAR, China. Tel.: +852 2819 9513; fax: +852 2855 9730.
E-mail address: grli@hkucc.hku.hk (G.-R. Li).
0006-2952/$ – see front matter © 2007 Elsevier Inc. All rights reserved.
doi:10.1016/j.bcp.2007.07.042

It was reported that BAPTA-AM inhibited neuronal Ca^{2+}-activated K^+ channel currents [9,10], and up-regulated the decreased cardiac sodium current (I_{Na}) density by chelating intracellular Ca^{2+} [4]. The human ether a-go-go-related gene (hERG) channels, referred to as Kv11.1 encoded by KCNH2 [11], is responsible for the rapidly activating delayed rectifier potassium channel current (I_{Kr}) in the heart. Dysfunction of the channel has been implicated in long QT syndrome that can predispose individuals to lethal arrhythmias. Either inherited mutations of hERG or hERG channel block by variety of medications can cause long QT syndrome [12,13]. It has been reported that human ether a-go-go gene (hEAG) potassium channels are regulated by intracellular Ca^{2+}/calmodulin [14,15]. The present study was initially designed to investigate whether hERG channels would be regulated by intracellular Ca^{2+} using the membrane permeable Ca^{2+}-chelator BAPTA-AM. We found that hERG channels were blocked by the application of BAPTA-AM in bath solution, and also a similar effect was observed in Kv1.5 and Kv1.3 channels stably expressed in HEK 293 cells.

2. Material and methods

2.1. Gene transfection and establishment of cell lines

The vector of hERG/pcDNA3 generously provided by Dr. G. Robertson (University of Wisconsin, Madison, WI, USA) [16] was transfected into HEK 293 cells (ATCC, Manassas, VA, USA) using 10 μl Lipofectamine 2000™ (Invitrogen, Hong Kong) with 4 μg hERG/pcDNA3 plasmid, and selected using 1000 μg/ml G418 (Sigma–Aldrich, St. Louis, MO). Colonies were picked with cloning cylinders and examined for channel expression by whole-cell current recordings as described previously [17]. The selected cell line stably expressing hERG channels was maintained in DMEM medium containing 400 μg/ml G418 (Sigma–Aldrich) and 10% fetal bovine serum.

The mutant hERG channels S631A and Y652A generously provided by Dr. S. Zhang (University of Manitoba, Winnipeg. MA, Canada) [18,19] were transiently expressed in HEK 293 cells. HEK 293 cells were seeded at 5×10^5 cells/60-mm-diameter dish. The cells were transiently transfected using 10 μl of Lipofectamine 2000™ with 4 μg of hERG mutant cDNA in pCDNA3 vector. After 24–48 h, 20–30% of cells expressed channels.

The vector of hKv1.3/pcDNA3 provided by Dr. O. Pongs (Institut fur Neurale Signalverarbeitung, Germany) [20] and the vector of hKv1.5/pBK_{CMV} provided by Dr. M Tamkun (Colorado State University, CO, USA) were separately transfected into HEK 293 cells using Lipofectamine 2000™, and selected with 1000 μg/ml G418. Colonies were picked with cloning cylinders and examined for channel expression by whole-cell current recordings as previously described [17]. The HEK 293 cell line stably expressing hKv1.5 or hKv1.3 was maintained in DMEM medium containing 400 μg/ml G418 (Sigma–Aldrich).

2.2. Solution and reagents

Tyrode solution contained (in mM): NaCl 140, KCl 5.0, $MgCl_2$ 1.0, $CaCl_2$ 1.8, NaH_2PO_4 0.33, HEPES 10.0, glucose 10, and pH adjusted to 7.3 with NaOH. When external K^+ concentration ($[K^+]_o$) was increased, equimolar external Na^+ was reduced (specified). The pipette solution contained (in mM): KCl 20, K-aspartate 110, $MgCl_2$ 1.0, HEPES 10, EGTA 5.0 (or 0.05 specified), and GTP 0.1, Na_2-phosphocreatine 5.0, Mg_2-ATP 5.0, with pH adjusted to 7.2 with KOH. In some experiments, the pipette EGTA was replaced by BAPTA (specified). BAPTA-AM (Calbiochem, UK) was prepared as 10–30 mM stock solutions in dimethyl sulfoxide (DMSO) and added to the bath solution at the indicated final concentrations, and the final concentration (0.1%) of DMSO had no effect on any channel current. All the chemicals were purchased from Sigma–Aldrich except for those specified.

2.3. Data acquisition and analysis

Cells on a coverslip were transferred to an open cell chamber (0.5 ml) mounted on the stage of an inverted microscope and superfused with Tyrode solution at ~2 ml/min. Experiments were performed at room temperature (21–22 °C). The whole cell patch-clamp technique was used as described previously [21]. Briefly, borosilicate glass electrodes (1.2 mm OD) were pulled with a Brown-Flaming puller (model P-97, Sutter Instrument Co., Novato, CA, USA) and had tip resistances of 2–3 MΩ when filled with the pipette solution. A 3-M KCl-agar salt bridge was used as reference electrode. Tip potentials were zeroed before the pipette touched the cell. After a gigaohm seal was obtained, the cell membrane was ruptured by gentle suction to establish whole-cell configuration to record hERG, Kv1.5, or Kv1.3 channel currents. Liquid junction potentials after membrane rupture between the external and pipette solutions (10.5 ± 0.3 mV) [22] were not corrected for all current recording. The membrane currents were recorded with an EPC-10 amplifier and Pulse software (HEKA, Lambrecht, Germany). Command pulses were generated by a 12-bit digital-to-analog converter controlled by Pulse software. Current signals at 2–5 kHz sampling rates were low-pass filtered at 5 kHz and stored on the hard disk of an IBM computer.

Values are presented as mean ± S.E.M. Nonlinear curve fitting was performed using Pulsefit (HEKA) and/or Sigmaplot (SPSS Science, Chicago, IL, USA). Paired and/or unpaired Student's *t*-tests were used to evaluate the statistical significance of differences between two group means. ANOVA was used for multiple groups. Values of $P < 0.05$ were considered statistically significant.

3. Results

3.1. Effects of BAPTA-AM on hERG channel current

Our initial purpose was to study whether the chelation of intracellular Ca^{2+} with external BAPTA-AM would affect hERG current (I_{hERG}), a pipette solution with low EGTA (0.05 mM) was used to record I_{hERG} in HEK 293 cells stably expressing hERG channels superfused with normal Tyrode solution. We found that I_{hERG} was rapidly inhibited by application of 10 μM BAPTA-AM in Tyrode solution, and the effect quickly recovered upon washout ($n = 5$, data not shown), suggesting

that the inhibition of I_{hERG} by BAPTA-AM is not likely related to the intracellular Ca^{2+} chelation.

Fig. 1A illustrates the time course of hERG tail current recorded in a representative cell with the voltage protocol shown in the inset using a pipette solution containing 5 mM EGTA. I_{hERG} did not change during dialysis of high EGTA pipette solution, while the current was rapidly inhibited by application of 10 μM BAPTA-AM in Tyrode solution. The effect reached a steady-state level within 2 min, and significantly reversed by washout for 3 min. Original current traces at corresponding time points are shown in right of the panel. Similarly, I_{hERG} recorded with a pipette solution containing

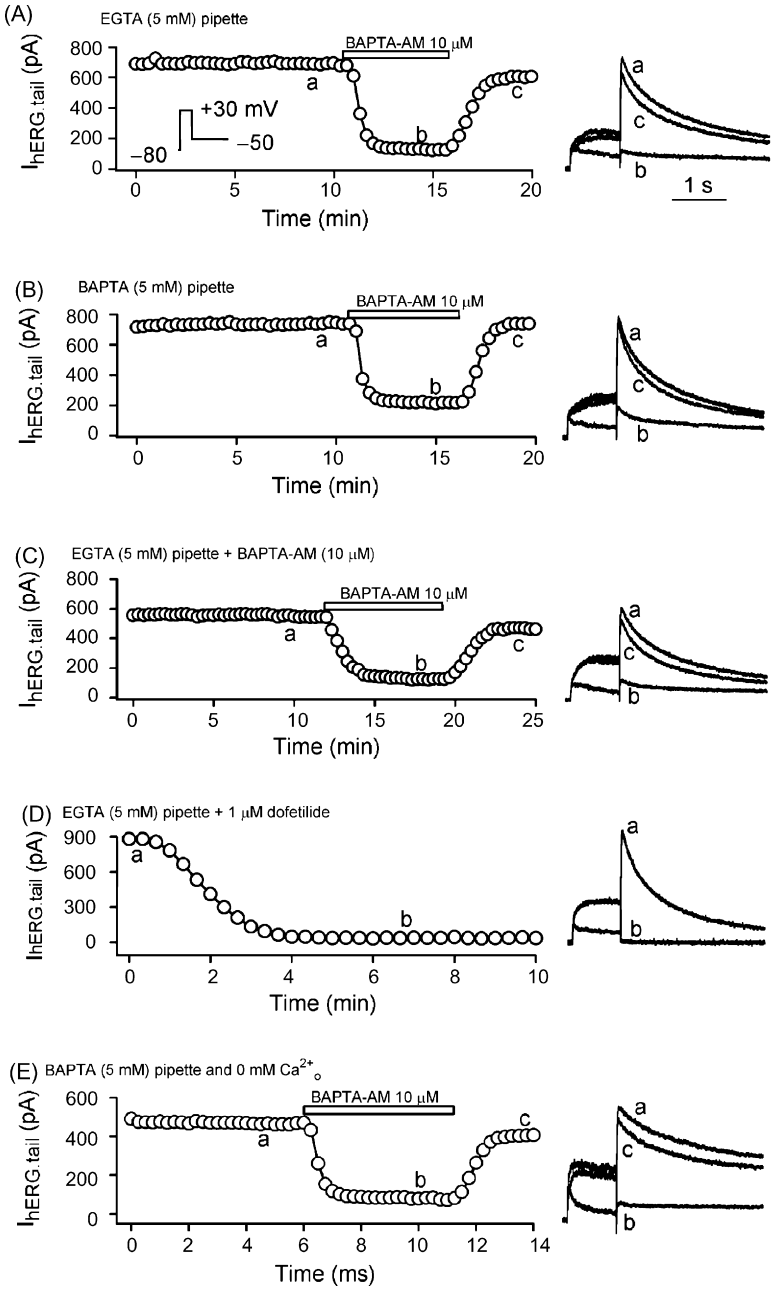

Fig. 1 – Inhibition of hERG channel current by BAPTA-AM. (A) Time course of hERG tail current recorded in a HEK 293 cell stably expressing hERG channels with a standard pipette solution containing 5 mM EGTA. Membrane current was elicited by a 1-s voltage step to +30 mV from a holding potential of –80 mV, then back to −50 mV (left *inset*) every 20 s. BAPTA-AM at 10 μM reversibly suppressed hERG channel current. (B) Time course of hERG tail current recorded in another cell stably expressing hERG channels with a pipette solution containing 5 mM BAPTA using the same protocol as in A. BAPTA-AM at 10 μM exhibits a similar inhibition of hERG current to that with 5 mM EGTA pipette solution. (C) Inclusion of 10 μM BAPTA-AM in pipette solution produced no effect on hERG channel current; however, extracellular application of BAPTA-AM caused a substantial reduction in hERG channel current. (D) Inclusion of 1 μM dofetilide in pipette solution produced a substantial reduction in hERG channel current. (E) Blockade of I_{hERG} by BAPTA-AM was not affected by removal of external Ca^{2+}. Original current traces at corresponding time points are shown in the right of each panel.

5 mM BAPTA also showed a rapid reduction with 10 μM BAPTA-AM superfusion, and the effect quickly reversed on washout (Fig. 1B). To investigate whether the inhibition of hERG channels by BAPTA-AM was related to the interaction with intracellular binding site(s) of the channels, we included 10 μM BAPTA-AM in the pipette solution containing 5 mM EGTA. The dialysis of BAPTA-AM did not affect I_{hERG}, and the extracellular application of 10 μM BAPTA-AM produced a reversible inhibition of I_{hERG} (Fig. 1C), similar results were obtained in a total of 3 cells. To exclude the possibility that

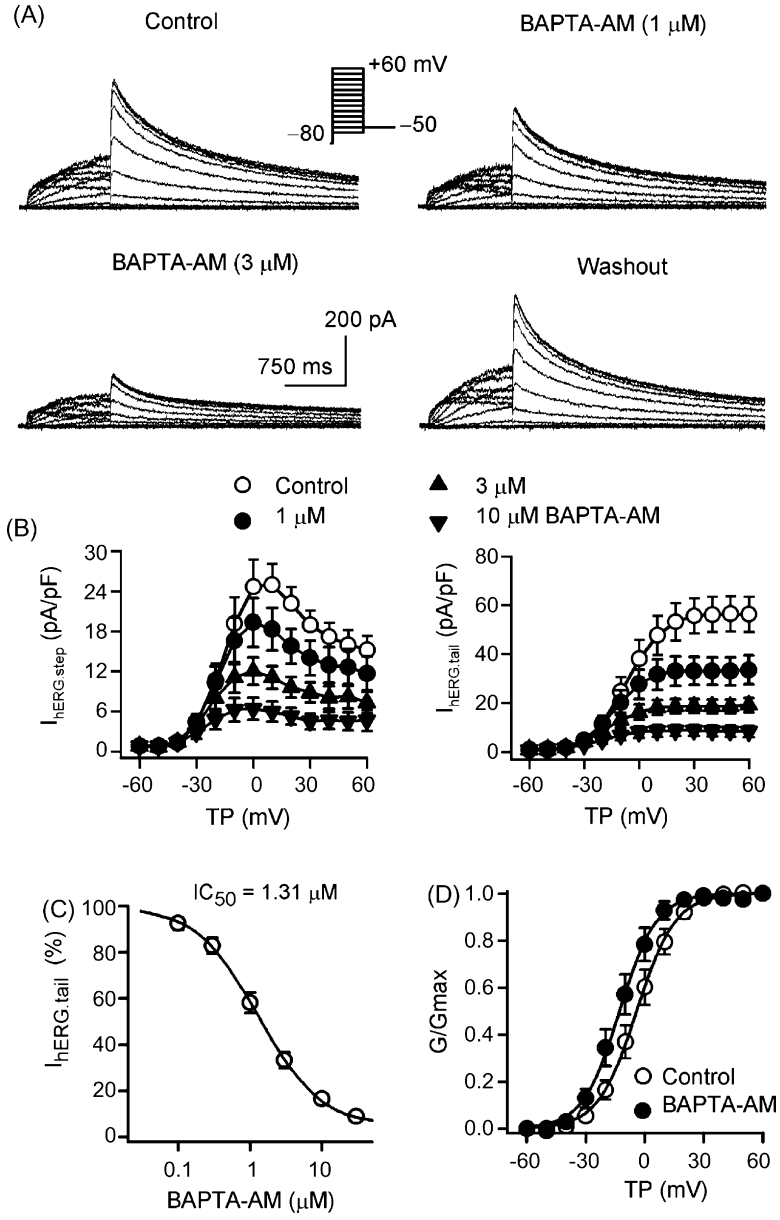

Fig. 2 – Concentration-dependent suppression of hERG channel current by BAPTA-AM. (A) Voltage-dependent hERG channel current was recorded in a typical experiment with 1-s voltage steps to between −60 and +60 mV from a holding potential of −80 mV, then back to −50 mV (inset) at 0.05 Hz in the absence and presence BAPTA-AM. BAPTA-AM at 1 and 3 μM inhibited voltage-dependent hERG channel step current ($I_{hERG.step}$) and tail current ($I_{hERG.tail}$), and the effect was reversed by washout. (B) Current-voltage (*I–V*) relationships of $I_{hERG.step}$ (left) and $I_{hERG.tail}$ (right) in the absence and presence of 1, 3, and 10 μM BAPTA-AM. I_{hERG} was substantially suppressed by 1–10 μM BAPTA-AM at potentials positive to −10 mV for $I_{hERG.step}$ (n = 8, $P < 0.05$ or 0.01 vs. control) or at potentials positive to 0 mV for $I_{hERG.tail}$ ($P < 0.05$ or $P < 0.01$ vs. control). $I_{hERG.step}$ was measured at the end of step from zero current, and $I_{hERG.tail}$ was measured at the peak of tail current. (C) Concentration response relationship of BAPTA-AM for inhibiting $I_{hERG.tail}$ (n = 6–9 experiments for each concentration). (D) Steady-state activation relationships of hERG channels were fitted to the Boltzmann distribution: $y = 1/\{1 + \exp[(V_m - V_{0.5})/S]\}$, where V_m is the membrane potential, $V_{0.5}$ is the midpoint, and S is the slope. The $V_{0.5}$ for activation conductance of hERG channels was −3.7 ± 2.8 mV for control and −12.2 ± 3.1 mV for 3 μM BAPTA-AM (n = 13, $P < 0.01$), while *S* was 7.9 ± 0.3 and 6.9 ± 0.3 mV for control and BAPTA-AM, respectively ($P > 0.05$).

incomplete drug dialysis from pipette solution induced a non-observable effect of BAPTA-AM, we included 1 μM dofetilide (an intracellular hERG channel blocker) in pipette solution. Dialysis of dofetilide caused a remarkable block (Fig. 1D). These results suggest that blockade of hERG channels by BAPTA-AM, not like dofetilide, is likely related to its interaction with the channels from outside of the cell.

In addition, a similar inhibition of I_{hERG} by 10 μM BAPTA-AM was observed (Fig. 1E) after removing external Ca^{2+}, similar results were obtained in other 6 cells. To study whether BAPTA would show a similar inhibitory effect on hERG channels, 10 μM BAPTA was added in the Ca^{2+}-free bath solution. A slight reduction (by $5.1 \pm 2.3\%$, $n = 5$, $P = 0.05$) of $I_{hERG.tail}$ was observed with 10 μM BAPTA (data not illustratively shown), and the effect was much weaker than that of BAPTA-AM ($78.1 \pm 2.9\%$, $P < 0.0001$ vs. BAPTA). These results indicate that BAPTA-AM blocks hERG channel in an external Ca^{2+} independent manner.

Concentration and voltage dependence of I_{hERG} was studied with 0.1–30 μM BAPTA-AM. Fig. 2A shows the effects of BAPTA-AM on voltage-dependent I_{hERG} recorded in a representative cell. BAPTA-AM at 1 and 3 μM substantially suppressed I_{hERG}, and the effect was reversed by washout. Fig. 2B illustrates current–voltage (I–V) relationships of hERG step current ($I_{hERG.step}$) and tail current ($I_{hERG.tail}$) before and after application of 1, 3, and 10 μM BAPTA-AM. Both $I_{hERG.step}$ and $I_{hERG.tail}$ were substantially blocked by BAPTA-AM in a concentration-dependent manner. The concentration–response relation (Fig. 2C) was fitted to the Hill equation: $E = E_{max}/[1 + (IC_{50}/C)^b]$, where E is the inhibition of current in percentage at concentration C, E_{max} is the maximum inhibition, IC_{50} is the concentration for a half-maximum action, and b is the Hill coefficient. The IC_{50} of BAPTA-AM for inhibiting $I_{hERG.tail}$ was 1.31 μM, Hill coefficient was 1.0, and E_{max} was 91%, and the IC_{50} for inhibiting $I_{hERG.step}$ was 1.10 μM, Hill coefficient was 1.07, and E_{max} was 88%.

Voltage dependence of hERG channel activation (G/G_{max}) was determined by normalizing $I_{hERG.tail}$ in the absence and presence of 3 μM BAPTA-AM (Fig. 2D). The G/G_{max} curves were fitted to a Boltzmann distribution to obtain midpoint ($V_{0.5}$) of activation potential and slope factor. The $V_{0.5}$ of hERG channel activation conductance was negatively shifted by 8.5 mV (from -3.7 ± 2.8 of control to -12.2 ± 3.1 mV, $n = 13$, $P < 0.01$) by 3 μM BAPTA-AM, and the slope factor was slightly decreased (7.9 ± 0.3 mV for control, 6.9 ± 0.3 mV for BAPTA-AM, $P > 0.05$).

Fig. 3A illustrates the voltage protocol and representative current traces used for determining voltage dependence of steady-state inactivation (availability) of hERG channels. After a 1-s pulse to +40 mV to activate the channels, the membrane voltage was stepped briefly to various test potentials and then to +40 mV. During the brief 20-ms pulses, the inactivation of hERG channels relieved rapidly to the steady-state level, and the initial current on stepping to +40 mV gave the relative number of open channels. Fig. 3B represents the initial current amplitude at +40 mV against the interpulse potentials in the absence and presence of 3 μM BAPTA-AM. At negative potentials, the currents decline because significant closing of channels occurs through deactivation. It was corrected for by extrapolating exponential falling phase measured in full at

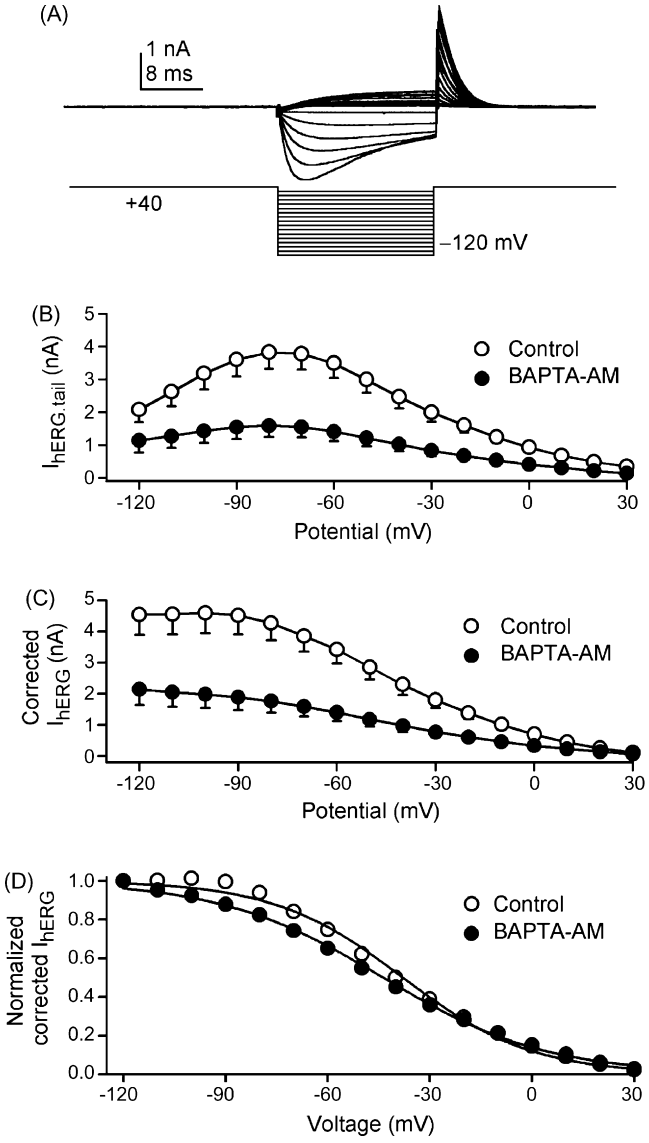

Fig. 3 – Effect of BAPTA-AM on steady-state inactivation of hERG channels. (A) Current recordings obtained with the protocol used to assess steady-state inactivation. After a 1-s inactivation step at +40 mV rapid inactivation of hERG channels was relieved by application of 20-ms test pulses to potentials ranging from −120 to +30 mV. (B) Steady-state inactivation of hERG channels. Peak outward currents (from A) elicited during the second step to +40 mV obtained in the absence and presence of 3 μM BAPTA-AM were plotted as a function of voltage steps. (C) Peak outward currents corrected for closing inactivation curves in the absence and presence of BAPTA-AM. (D) Normalized inactivation curves of corrected hERG current in the absence and presence of BAPTA-AM fitted to a Boltzmann distribution.

end of the procedure back to the start of the negative voltage step, and applying the same relative correction to the initial outward current as described previously by Smith et al. [24]. Fig. 3C shows the corrected current by extrapolating the exponential decay phase back to the start of the negative

voltage step and applying the same relative correction to the initial outward current as described previously [23,24]. The normalized inactivation curves (Fig. 3D) of corrected I_{hERG} were fitted to a Boltzmann distribution. The $V_{0.5}$ of hERG channel inactivation was negatively shifted by 6.1 mV with 3 μM BAPTA-AM (from −37.9 ± 2.0 mV of control to −44.0 ± 1.6 mV, $n = 8$, $P < 0.05$), and slope factor was −18.8 ± 0.7 for control, and −24.0 ± 1.3 mV for BAPTA-AM ($P < 0.05$).

3.2. *Open channel block of hERG channels by BAPTA-AM*

The short voltage pulses above could not reflect the development of hERG channel block. Therefore, the time-dependence of development of blocking I_{hERG} by BAPTA-AM was investigated using a 10-s step to 0 mV from a holding potential of −80 mV (upper panel of Fig. 4A). The protocol was applied in control, and discontinued during 3 min exposure to 3 μM BAPTA-AM (holding potential −80 mV), then reapplied in the presence of drug. Fig. 4A shows representative I_{hERG} traces (lower panel) during a 10-s step to 0 mV recorded in control and after 3 μM BAPTA-AM. BAPTA-AM inhibited I_{hERG} less at beginning of the current activation than at end of depolarization step, showing an apparent current inactivation, consistent with open channel block.

To analyze the onset of open channel block, the time course for the development of inhibition by BAPTA-AM was exponentially fitted as in Fig. 4B. The drug-sensitive current was expressed as a proportion of the current in the absence of the drug ($(I_C - I_B)/I_C$), where I_C and I_B are the currents in the absence and presence of BAPTA-AM. Drug-induced block was then plotted as a function of time after the onset of the pulse [25]. The block was found to develop in a time-dependent fashion, with an exponential onset as shown by the curve fit in the Fig. 4B. Time constant of the rate of block development was 1606.3 ± 158.0 ms with 3 μM BAPTA-AM ($n = 7$), and the time-dependent onset of block is consistent with open channel block.

The time course for the development of BAPTA-AM block of hERG channels was also assessed using an envelope of tail test [26]. Cells were held at a holding potential of −80 mV and pulsed to depolarizing voltage (+30 mV) for a variable duration from 50 to 4950 ms in 250-ms increments. $I_{hERG.tail}$ was recorded upon repolarization to −50 mV (upper panel of Fig. 4C). The envelope tail test was performed in the same cell before and after addition of 3 μM BAPTA-AM. The onset of hERG channel block was expressed by plotting the relative tail current as a function of the pulse duration (lower panel of Fig. 4C). The envelope tail current with 3 μM BAPTA-AM was expressed relative to control (Fig. 4D), and the relative tail current decayed in a pulse duration-dependent manner. The time course of this decay was fitted to a single exponential function. The onset of hERG channel block by 3 μM BAPTA-AM developed rapidly with a time constant of 328.5 ± 9.9 ms at +30 mV ($n = 5$). In addition, the inactivation of hERG channels would be significant with the long step protocol and envelop test tail protocol. Therefore, it should be noted that the development of hERG channel inactivation likely contributes to the development of blockade with these protocols.

Tonic block of hERG channel current by BAPTA-AM was estimated by the initial value of the relative tail current

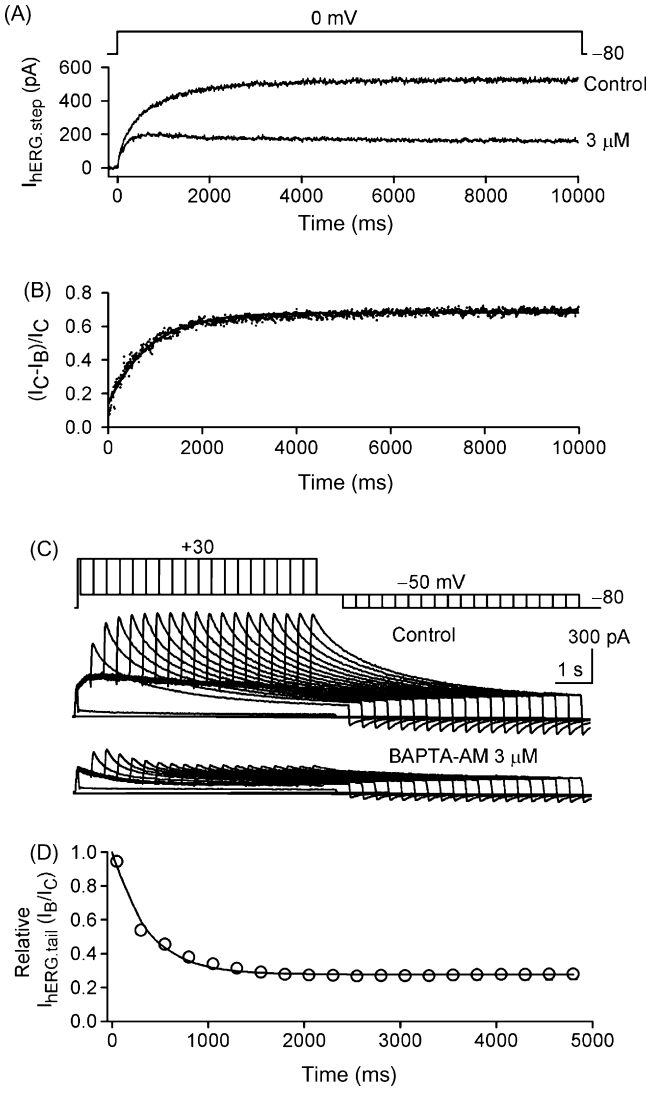

Fig. 4 – Onset of hERG channel current block by BAPTA-AM using a long step pulse protocol and an envelope of tails protocol. (A) Voltage-clamp pulse protocol and representative recordings of hERG current before and after exposure of cell to 3 μM BAPTA-AM. The current was substantially inhibited by 3 μM BAPTA-AM, and similar results were obtained in a total of 6 cells. (B) Drug-sensitive current expressed as a proportion of the current in the absence and presence of 3 μM BAPTA-AM. Raw data (points) were fitted to a single exponential function with a time constant of 865 ms. (C) Envelope tail protocol and representative hERG current before (control) and after application of 3 μM BAPTA-AM. (D) A plot of the onset of current block expressed as relative tail current. The time-dependent decay in relative tail current was fitted to a single exponential function. The relative steady state value of the current was 0.27 ($n = 8$).

activated by the envelope protocol. The initial relative tail current (at 50 ms) with 3 μM BAPTA-AM was 94.5 ± 2.3%, therefore actual tonic block of hERG channels by 3 μM BAPTA-AM was minimal. Taken together, these results indicate that BAPTA-AM does not bind to hERG channels in the resting state,

and activation is required for BAPTA-AM to block hERG channels.

3.3. *Effects of alanine substitution of S631 and Y652 on BAPTA-AM*

To further study BAPTA-AM block of hERG channels, two hERG mutants, S631A and Y652A, were evaluated. The S631A mutation lies near the external mouth of the channel pore, and the Y652A mutation is on the S6 helices of the hERG channel, both mutations have been shown to dramatically attenuate I_{hERG} block by a number of drugs [27–30]. To test whether BAPTA-AM also binds to the outer mouth of the channel pore or within the inner cavity of the channel, the inhibition of S631A and Y652A hERG channels by BAPTA-AM was measured in HEK 293 cells. The results in Fig. 5 show that the mutant Y652A significantly attenuates hERG channel block, while the mutant S631A dramatically reduces hERG channel block by BAPTA-AM. At test potential of +30 mV, BAPTA-AM (10 μM) inhibited $I_{hERG.step}$ and $I_{hERG.tail}$ by 84.1 ± 2.1% and 85.8 ± 1.2% for wild type channels, 66.5 ± 2.5 ($n = 6$, $P < 0.01$ vs. wild type) and 69.8 ± 5.6% ($P < 0.05$ vs. wild type) for Y652A channels, and 34.8 ± 4.1% ($n = 5$, $P < 0.01$ vs. wild type) and 24.6 ± 3.1% ($P < 0.01$ vs. wild type) for S631A channels. The inhibition of S631A channels by BAPTA-AM was weaker than that of Y652A channels ($P < 0.01$). Because the maximum soluble concentration of BAPTA-AM was 100 μM in our working solution, the E_{max} of BAPTA-AM for inhibiting the mutant channels could not reach to the similar maximum value to that in wild type channels. Therefore, we did not compare the IC_{50} value of BAPTA-AM in wild type and mutant channels. BAPTA-AM at 100 μM produced an E_{max} of $I_{hERG.tail}$ inhibition of 40.5 ± 8.8% for S631A mutant, and 72.8 ± 1.8% for Y652A mutant.

The above results with the non-inactivating mutant S631A suggest that inactivation is likely involved in the blockade of hERG channels by BAPTA-AM. To test this, we increased $[K^+]_o$ to 20 mM to reduce the inactivation of wild type hERG channels [28;30]. Using BAPTA-AM (0.1–100 μM), we found that the IC_{50} of BAPTA-AM for inhibiting $I_{hERG.tail}$ was 2.93 μM under conditions of 20 mM $[K^+]_o$ (data not illustratively shown), suggesting the efficacy of channel block slightly decreased (IC_{50} = 1.31 μM with 5 mM K^+_o) as $[K^+]_o$ increased. This result suggests that channel inactivation is partially involved in the blockade of hERG channels by BAPTA-AM.

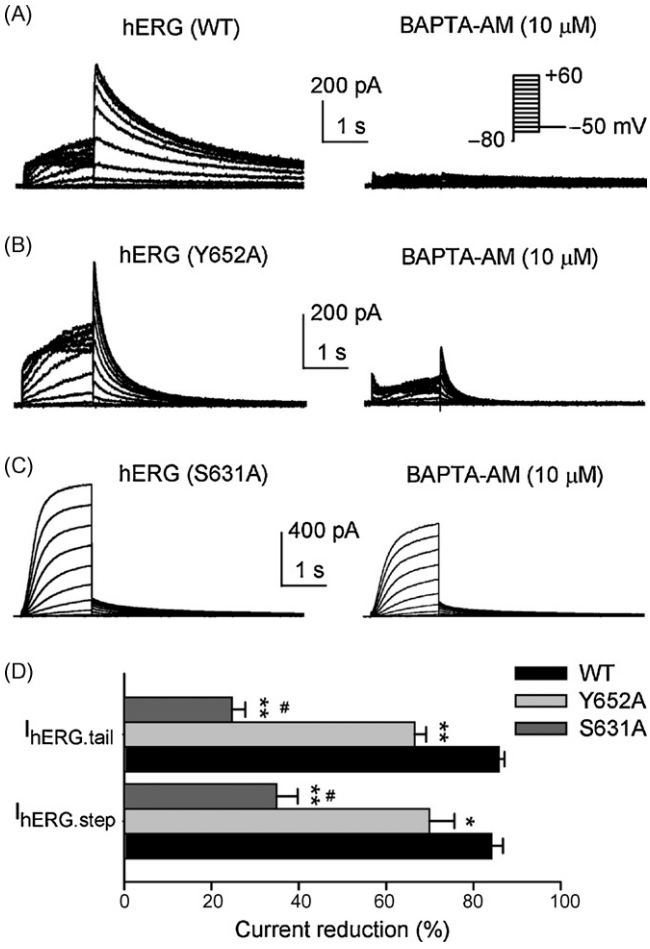

Fig. 5 – Effects of alanine substitution of S631 and Y652 on BAPTA-AM. (A) Current traces recorded in a HEK 293 cell stably expressing Wild type (WT) hERG channels in the absence and presence of 10 μM BAPTA-AM. (B) Representative current traces recorded in a HEK 293 cell transiently expressing hERG Y652A channels before and after 10 μM BAPTA-AM. (C) Current traces recorded in a HEK 293 cell transiently expressing hERG S631A channels before and after 10 μM BAPTA-AM. D. Percent reduction of the current after application of 10 μM BAPTA-AM in hERG wild type ($n = 8$), hERG Y652A ($n = 5$), and hERG S631A ($n = 5$) channels. $^{*}P < 0.05$; $^{**}P < 0.01$ vs. wild type hERG channels. $^{\#}P < 0.01$ vs. Y652A mutant.

3.4. *Effects of BAPTA-AM on hKv1.3 and hKv1.5 channels*

Previous studies showed that BAPTA-AM directly inhibited the delayed rectifier K^+ channel currents in rat neurons [31] and bovine chromaffin cells [32]. In the present study, HEK 293 cells stably expressing hKv1.3 or hKv1.5 were employed to determine whether BAPTA-AM suppressed cloned human delayed rectifier K^+ channels. Fig. 6 illustrates the effects of BAPTA-AM on hKv1.3. BAPTA-AM at 3 μM inhibited Kv1.3 current and increased inactivation process of the current, the inhibition reversed on washout (Fig. 6A). Fig. 6B displays the *I–V* relationships of hKv1.3 in the absence and presence of 1 and 10 μM BAPTA-AM. BAPTA-AM significantly suppressed hKv1.3 at test potentials from −30 to +60 mV ($n = 5$, $P < 0.05$ or $P < 0.01$ vs. control), and stronger inhibition was observed at more positive potentials. The concentration–response relationship of BAPTA-AM for inhibiting hKv1.3 is illustrated in Fig. 6C. The curve was fitted to a Hill equation; the IC_{50} of BAPTA-AM for inhibiting hKv1.3 was 1.45 μM, Hill co-efficient was 0.6, and E_{max} was 83%.

In another set of experiments, we included 10 μM BAPTA-AM in pipette solution. Dialysis of BAPTA-AM did not show any inhibitory effect on hKv1.3 channels, while bath application of 10 μM produced a substantial suppression of hKv1.3 in the same cells ($n = 4$, data not illustratively shown), suggesting that the block of hKv1.3 channels by BAPTA-AM, as in hERG

channels, is likely related to its interaction with the channels from the outside of cell.

The increased inactivation of hKv1.3 channels observed in Fig. 6A and D suggests that the effect of BAPTA-AM is due to open channel block. To analyze the onset of open channel block, the drug-sensitive current was expressed as a proportion of the current in the absence of BAPTA-AM as described previously [25]. Drug-induced block was then plotted as a function of time after the onset of the pulse. The block was found to develop in a time-dependent fashion with an exponential onset as shown by the curve fits in the Fig. 6E. The rate of block development increased as concentration increased; average time constants were 111.3 ± 9.0 and 61.5 ± 10.8 ms at 1 and 3 μM BAPTA-AM ($n = 6$, $P < 0.05$) respectively. The time-dependent onset of block is also consistent with open channel blocking mechanism.

The effects of BAPTA-AM on hKv1.5 are illustrated in Fig. 7. BAPTA-AM reversibly inhibited hKv1.5, and increased inactivation of the current (Fig. 7A). Fig. 7B displays the *I–V* relationships of hKv1.5 in the absence and presence of 1 and 10 μM BAPTA-AM. BAPTA-AM significantly suppressed

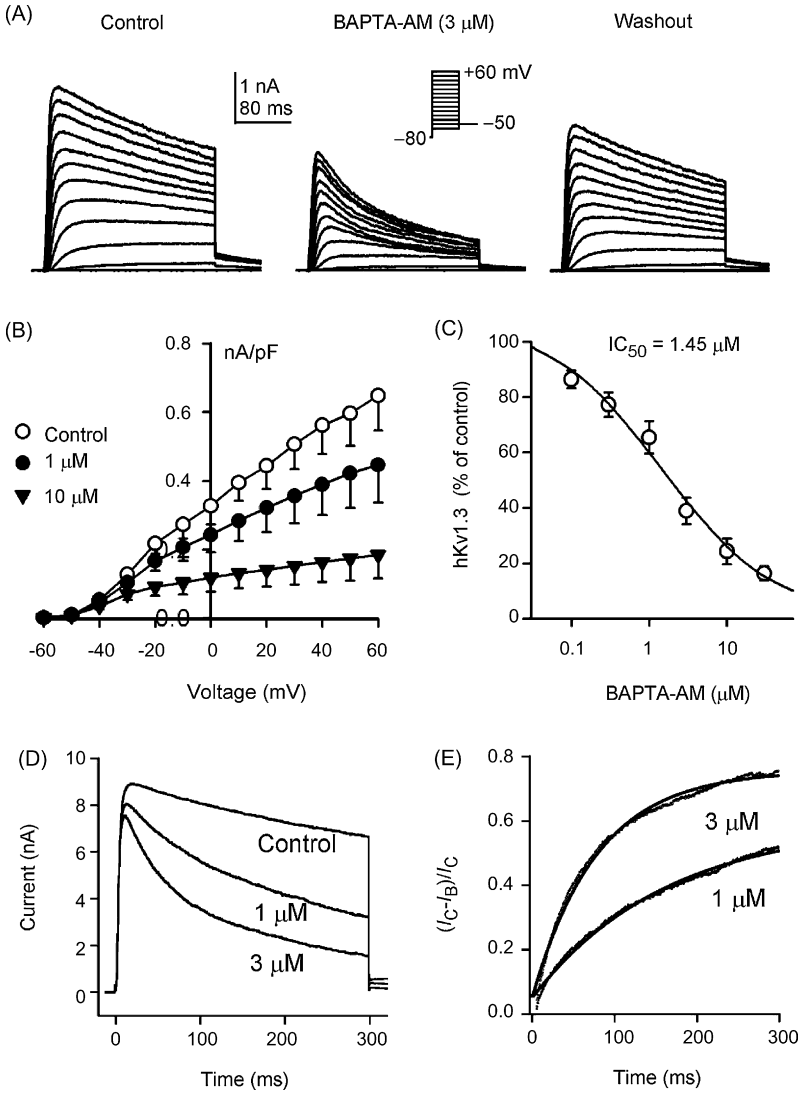

Fig. 6 – Open channel block on hKv1.3 by BAPTA-AM. (A) Kv1.3 current recorded in a representative HEK 293 cell stably expressing hKv1.3 channels using 300-ms voltage steps to voltages between −60 and +60 mV from a holding potential of –80 mV (*inset*) at 0.1 Hz in the absence and presence of 3 μM BAPTA-AM. BAPTA-AM inhibited the current amplitude, and accelerated inactivation process of the current, and the effect was partially reversed by washout. (B) *I–V* relationships of hKv1.3 (measured at end of the depolarization steps from the zero current) in absence and presence of 1 and 10 μM BAPTA-AM. (C) Concentration response relationship of BAPTA-AM for inhibiting hKv1.3 channels ($n = 5$–7 cells for each concentration). (D) Representative hKv1.3 traces recorded with a 300-ms pulse to +50 mV from a holding potential of −80 mV in a typical experiment in the absence and presence of 1 and 3 μM BAPTA-AM. The current inhibition by BAPTA-AM was stronger at the end of voltage step than that in the beginning of voltage step. (E) Drug-sensitive current expressed as a proportion of the current in the absence and presence of 1 and 3 μM BAPTA-AM. Raw data (points) were fitted to a single exponential function with time constants of 115.6 and 58.9 ms, respectively for 1 and 3 μM BAPTA-AM ($n = 6$, $P < 0.05$).

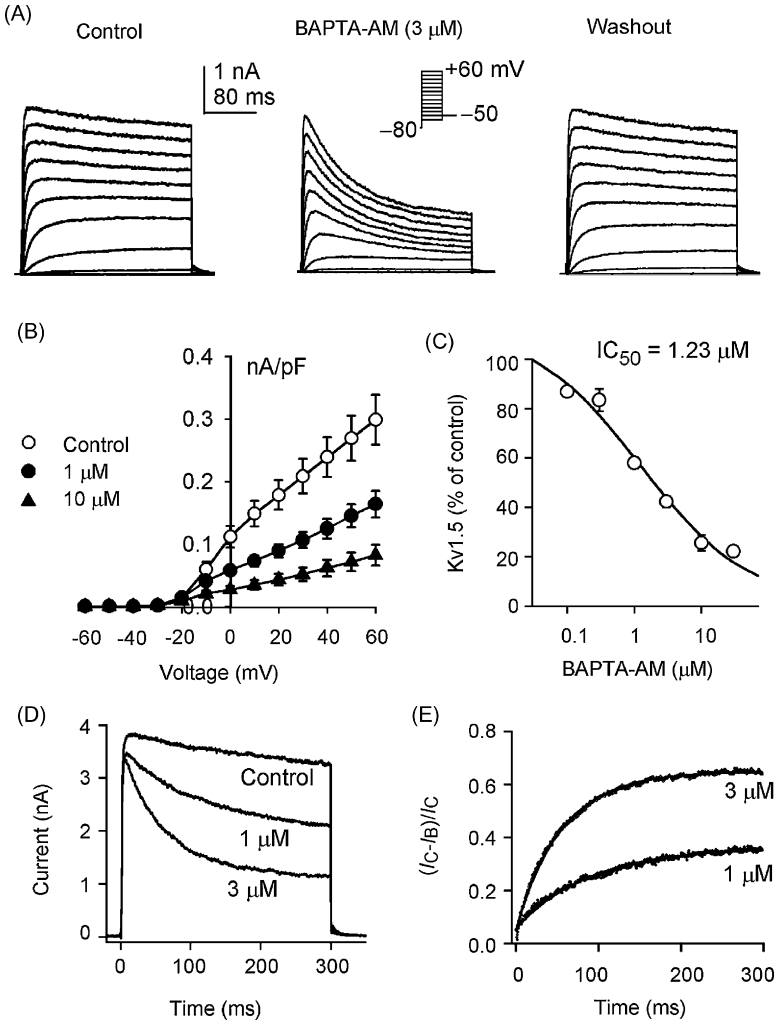

Fig. 7 – Open channel block of hKv1.5 by BAPTA-AM. (A) Kv1.5 current recorded in a representative HEK 293 cell stably expressing hKv1.5 channels with 300-ms voltage steps to between −60 and +60 mV from a holding potential of −80 mV (*inset*) at 0.1 Hz in the absence and presence of 3 μM BAPTA-AM. BAPTA-AM inhibited the current amplitude, and accelerated inactivation process of the current, and the effect was partially reversed by washout. (B) *I–V* relationships of hKv1.5 (measured at end of the depolarization steps from the zero current) in the absence and presence of 1 and 10 μM BAPTA-AM. (C) Concentration response relationship of BAPTA-AM for inhibiting hKv1.5 channels (n = 5–9 cells for each concentration). (D) Representative hKv1.5 traces recorded with a 300-ms pulse to +50 mV from a holding potential of −80 mV in a typical experiment in the absence and presence of 1 and 3 μM BAPTA-AM. The current inhibition by BAPTA-AM was stronger at the end of voltage step than that in the beginning of voltage step. (E) Drug-sensitive hKv1.5 current expressed as a proportion of the current in the absence and presence of 1 and 3 μM BAPTA-AM. Raw data (points) were fitted to a single exponential function with time constants of 59.7 and 46.1 ms respectively for 1 and 3 μM BAPTA-AM (n = 6, $P < 0.05$).

hKv1.5 at test potentials from −10 to +60 mV (n = 11, $P < 0.05$ or $P < 0.01$ vs. control). The concentration–response relationship of BAPTA-AM is illustrated in Fig. 7C. The curve was fitted to a Hill equation, and the IC_{50} of BAPTA-AM for inhibiting hKv1.5 was 1.23 μM, Hill co-efficient was 0.6, and E_{max} was 78%.

In addition, inclusion of 10 μM BAPTA-AM in pipette solution did not exhibit any inhibitory effect on hKv1.5 channels, while bath application of 10 μM produced a remarkable suppression of hKv1.5 channels in the same cells (n = 5, data not illustratively shown), indicating that the inhibition of hKv1.5 channels by BAPTA-AM, most likely as in hERG and hKv1.3 channels, is involved in its interaction with the channel molecule from the exterior.

The increased inactivation of hKv1.5 inactivation (Fig. 7A and D) implies an open channel block action with BAPTA-AM. The onset of open channel block was analyzed by exponentially fitting the drug-sensitive current (Fig. 7E). The block developed in a time-dependent fashion with an exponential onset. The rate of block development increased as concentration increased; average time constants were 60.4 ± 6.3 and 45.9 ± 5.9 ms, respectively, at 1 and 3 μM BAPTA-AM (n = 7, $P < 0.05$). The time-dependent onset of block for hKv1.5 is also consistent with open channel block.

3.5. *Effects of EGTA-AM on hERG, hKv1.3, and hKv1.5 channels*

To investigate whether EGTA-AM would exhibit an inhibitory action on ion channels, the effects of EGTA-AM on hERG, hKv1.3, and hKv1.5 channels were determined in HEK 293 cell lines. EGTA-AM at 50 μM substantially inhibited both $I_{hERG.step}$ and $I_{hERG.tail}$ in HEK 293 cell line stably expressing hERG channels, and the effect was partially reversed by washout. At test potential of +30 mV, $I_{hERG.step}$ and $I_{hERG.tail}$ were reduced from 237 ± 21.3 and 543.3 ± 52.6 pA in control to 100.9 ± 18.0 and 147.8 ± 8.8 pA ($n = 6$, $P < 0.01$ vs. control) with 50 μM EGTA-AM, and recovered to 191.7 ± 21.8 and 258.3 ± 30.6 pA ($P < 0.05$ vs. EGTA-AM) after washout for 3 min. However, EGTA at 50 μM had no inhibitory effect on hERG channels ($n = 5$, data not shown).

EGTA-AM at 50 μM also substantially suppressed Kv1.3 channel current, and increased inactivation of the current. At test potential of +30 mV, hKv1.3 channel current was decreased from 4.6 ± 1.2 nA in control to 1.1 ± 0.4 nA ($n = 5$, $P < 0.01$ vs. control) with 50 μM EGTA-AM, and recovered to 2.8 ± 0.9 nA ($P < 0.05$ vs. EGTA-AM) after washout.

EGTA-AM at 50 μM showed a weak inhibition of hKv1.5, and also accelerated inactivation process of the current, and the effect was fully reversed on washout. At test potential of +30 mV, hKv1.5 was reduced from 2.6 ± 0.5 nA in control to 1.9 ± 0.4 nA with 50 μM EGTA-AM ($n = 8$, $P < 0.01$ vs. control), and recovered to 2.5 ± 0.6 nA ($P < 0.01$ vs. EGTA-AM) after washout.

4. Discussion

BAPTA-AM is a well known membrane permeable Ca^{2+} chelator widely used as an intracellular Ca^{2+} sponge to control intracellular Ca^{2+} concentration in the studies on intracellular Ca^{2+} signal regulation of cellular physiological and biological functions [2,3] including ion channel activity [4–7,33]. In addition, it was reported that BAPTA-AM inhibited protein kinase C in macrophages [34]. Moreover, BAPTA-AM was found to directly inhibit delayed rectifier K^+ currents in rat neurons [31]. It also blocked delayed rectifier and Ca^{2+} activated K^+ currents without affecting transient outward K^+ current (I_A), Ca^{2+} current, and Na^+ current in bovine chromaffin cells [32]. The present study demonstrated novel information that in addition to blockade of hKv1.3 and hKv1.5 channels, BAPTA-AM directly blocked hERG channels stably expressed in HEK 293 cells.

Our results demonstrated that the blockade of hERG channels by BAPTA-AM was not related to the buffer of intracellular Ca^{2+}. First, the inhibition of hERG channels by BAPTA-AM was independent of intracellular and external Ca^{2+}, because the effect was not affected by buffering intracellular Ca^{2+} with 5 mM EGTA (Fig. 1A) or 5 mM BAPTA (Fig. 1B) in pipette solution or removing external Ca^{2+}. Second, the inhibitory effect rapidly reached a steady-state level after exposure, and quickly reversed on washout. Third, the intracellular application of BAPTA-AM did not show inhibition of hERG channels, while external application of equimolar BAPTA-AM exhibited a substantial and reversible suppression of hERG channels (Fig. 1C), suggesting that the block of hERG channels by BAPTA-AM is related to its interaction with channel molecule from the exterior. On the other hand, our results strongly support the notion that hERG channels, which is different from human ether a-ago-go gene (hEAG) channels [14], are not regulated by intracellular Ca^{2+} and/or Ca^{2+}-related kinases (e.g. calmodulin).

BAPTA (10 μM), however, showed a very weak blocking effect on hERG channels (5% at +30 mV), compared with equimolar of BAPTA-AM (78%), which suggests that the combination of BAPTA with AM-ester molecule exhibits a strong efficacy of channel block. This phenomenon may also be applicable for EGTA. EGTA at 50 μM had no effect on hERG channels, while equimolar EGTA-AM significantly inhibited the channel current, although its effect was weaker than that of BAPTA-AM. The structure differences between BAPTA and EGTA may have contributed to the differential effects of these two compounds

BAPTA-AM inhibited hERG channels in a concentration-dependent manner with an IC_{50} of 1.3 μM (Fig. 2), and the concentration was much lower than those used for buffering intracellular Ca^{2+} in other systems [35–39], which further supports the notion that BAPTA-AM inhibits I_{hERG} by directly blocking hERG channels.

BAPTA-AM showed a potent and rapid block of hERG channels expressed in HEK 293 cells (Figs. 1 and 2). Block of hERG channels by BAPTA-AM exhibited the properties typical of open-channel blocker (Fig. 4). However, possible contribution of channel inactivation could not be excluded for the development of channel blockade. Tonic block of hERG current by BAPTA-AM (3 μM) was minimal (Fig. 4), suggesting that BAPTA-AM has a little affinity with channels in the closed or resting states. The blocking effect increased significantly at voltages more positive than +10 mV which elicit maximal hERG channel activation (Fig. 2B), and developed in response to a longer voltage pulse (Fig. 4A and B), and/or envelope voltage protocol, indicating that channel opening is required for the block of hERG channels by BAPTA-AM.

In the presence of BAPTA-AM, the $V_{0.5}$ for maximal activation of hERG channel was shifted to more negative potentials (Fig. 2D), suggesting that BAPTA-AM, like other hERG channel blockers (e.g. mesoridazine, fluvoxamine, clemastine) [29,40,41], affects the activation gating of hERG channels. In addition, the $V_{0.5}$ of steady-state inactivation was also negatively shifted by BAPTA-AM (Fig. 3), indicating that the inactivation gating of hERG channels was affected by BAPTA-AM.

A dramatically reduced blocking effect in the inactivation-deficient mutant S631A of hERG channels (Fig. 5) suggests that the channel inactivation is likely required for BAPTA-AM block of hERG channels as observed in several studies using cardiac or non-cardiac agents [28,30,42]. However, the inactivation reduction with increasing external K^+ concentration induced only a slight decrease of the efficacy of hERG channel block by BAPTA-AM, and is not strong as those observed in several cardiac agents [28,30], this supports the notion that the blockade of hERG channels relies on both the channel inactivation and binding to the outer mouth of the channels.

A weaker inhibition of hERG channels was observed in Y652A with the same concentration of BAPTA-AM (10 μM) (Fig. 5). Generally, agents (e.g. mesoridazine, clofilium, ketoconazole, etc.) that affect this residue and mutants of this residue exert their blocking action by crossing the membrane and entering the channel cavity from the cell interior [43–46]. However, the internally applied BAPTA-AM, not like dofetilide (Fig. 1D), had no effect on hERG channels (Fig. 1C). A possible explanation is that BAPTA-AM is probably an exceptional case different from other hERG channel blockers, and may bind to the central cavity of the gating channels from the exterior. Otherwise, the mutation of hERG channels may have directly altered channel affinity for this compound.

BAPTA-AM exhibited an open channel block of delayed rectifier K^+ channels in rat neurons [31] and bovine chromaffin cells [32]; however, it had no effect on I_A [31]. BAPTA-AM inhibited hKv1.3 and hKv1.5 channels stably expressed in HEK 293 cells in a concentration-dependent manner with IC_{50}s of 1.45 and 1.23 μM, respectively. Blockade of these two types of Kv channels by BAPTA-AM was also dependent on channel opening (Figs. 5 and 6) and related to its interaction with the channels from the exterior. The concentrations used in the present observation for channel blocking are significantly lower than those in neurons [31] and chromaffin cells [32]. The difference is likely related to the cloned human Kv channels (i.e. alpha-subunits) expressed in HEK 293 cells vs. the native animal Kv channels (i.e. whole channel assemblage).

Previous studies reported that hERG, Kv1.3 and Kv1.5 channels could be regulated by PKC [47–51], and BAPTA-AM was reported to inhibit PKC [34]. The present observation was involved in the study upon effect of PKC on these channels. However, possible effects of PKC could be excluded in the present observation because no effect was observed for these channels when BAPTA-AM was included in pipette solution. Collectively, our results support the notion that BAPTA-AM directly blocks hERG, Kv1.3 and Kv1.5 channels stably expressed in HEK 293 cells. In addition, EGTA-AM showed a blocking property similar to that of BAPTA-AM in hERG, Kv1.3 and Kv1.5 channels, although its efficacy is weaker than that of BAPTA-AM.

In summary, the membrane permeable Ca^{2+} chelator BAPTA-AM (also EGTA-AM), in addition to the inhibition of hKv1.3 and hKv1.5 channels, directly blocks hERG channels. These effects are not related to intracellular chelation.

Acknowledgement

This study was supported by Sun Chieh Yeh Heart Foundation of Hong Kong. The authors thank Dr. G. Robertson (University of Wisconsin-Madison, WI, USA) for providing the vector of hERG/pcDNA3; Dr. S. Zhang (University of Manitoba, Winnipeg. MA, Canada) for providing the hERG channel mutants S631A and Y652A; Dr. O. Pongs (Institut fur Neurale Signalverarbeitung, Germany) for providing the vector of hKv1.3/pcDNA3; and Dr. M. Tamkun (Colorado State University, CO, USA) for providing the vector of hKv1.5/pBK_{CMV}.

REFERENCES

[1] Tsien RY. A non-disruptive technique for loading calcium buffers and indicators into cells. Nature 1981;290:527–8.
[2] Bissonnette M, Tien XY, Niedziela SM, Hartmann SC, Frawley Jr BP, Roy HK, et al. 1,25(OH)2 vitamin D3 activates PKC-alpha in Caco-2 cells: a mechanism to limit secosteroid-induced rise in $[Ca^{2+}]_i$. Am J Physiol 1994;267:G465–75.
[3] Jiang S, Chow SC, Nicotera P, Orrenius S. Intracellular Ca^{2+} signals activate apoptosis in thymocytes: studies using the $Ca(^{2+})$-ATPase inhibitor thapsigargin. Exp Cell Res 1994;212:84–92.
[4] Guo J, Zhan S, Somers J, Westenbroek RE, Catterall WA, Roach DE, et al. Decrease in density of I_{Na} is in the common final pathway to heart block in murine hearts overexpressing calcineurin. Am J Physiol 2006;291:H2669–7.
[5] Perrier E, Perrier R, Richard S, Benitah JP. Ca^{2+} controls functional expression of the cardiac K^+ transient outward current via the calcineurin pathway. J Biol Chem 2004;279:40634–9.
[6] Bodding M, Flockerzi V. Ca^{2+} dependence of the Ca^{2+}-selective TRPV6 channel. J Biol Chem 2004;279:36546–52.
[7] Bugaj V, Alexeenko V, Zubov A, Glushankova L, Nikolaev A, Wang Z, et al. Functional properties of endogenous receptor- and store-operated calcium influx channels in HEK293 cells. J Biol Chem 2005;280:16790–7.
[8] Rao US, Baker JM, Pluznick JL, Balachandran P. Role of intracellular Ca^{2+} in the expression of the amiloride-sensitive epithelial sodium channel. Cell Calcium 2004;35:21–8.
[9] Niesen C, Charlton MP, Carlen PL. Postsynaptic and presynaptic effects of the calcium chelator BAPTA on synaptic transmission in rat hippocampal dentate granule neurons. Brain Res 1991;555:319–25.
[10] Tymianski M, Wallace MC, Spigelman I, Uno M, Carlen PL, Tator CH, et al. Cell-permeant Ca^{2+} chelators reduce early excitotoxic and ischemic neuronal injury in vitro and in vivo. Neuron 1993;11:221–35.
[11] Gutman GA, Chandy KG, Adelman JP, Aiyar J, Bayliss DA, Clapham DE, et al. International Union of Pharmacology. XLI. Compendium of voltage-gated ion channels: potassium channels. Pharmacol Rev 2003;55:583–6.
[12] Tseng GN. I_{Kr}: the hERG channel. J Mol Cell Cardiol 2001;33:835–49.
[13] Sanguinetti MC, Mitcheson JS. Predicting drug-hERG channel interactions that cause acquired long QT syndrome. Trends Pharmacol Sci 2005;26:119–24.
[14] Ziechner U, Schonherr R, Born AK, Gavrilova-Ruch O, Glaser RW, Malesevic M, et al. Inhibition of human ether a go-go potassium channels by Ca^{2+}/calmodulin binding to the cytosolic N- and C-termini. FEBS J 2006;273:1074–86.
[15] Schonherr R, Lober K, Heinemann SH. Inhibition of human ether a go-go potassium channels by Ca(2+)/calmodulin. EMBO J 2000;19:3263–71.
[16] Trudeau MC, Warmke JW, Ganetzky B, Robertson GA. HERG, a human inward rectifier in the voltage-gated potassium channel family. Science 1995;269:92–5.
[17] Dong MQ, Lau CP, Gao Z, Tseng GN, Li GR. Characterization of recombinant human cardiac KCNQ1/KCNE1 channels (I (Ks)) stably expressed in HEK 293 cells. J Membr Biol 2006;210:183–92.
[18] Guo J, Gang H, Zhang S. Molecular determinants of cocaine block of human ether-a-go-go-related gene potassium channels. J Pharmacol Exp Ther 2006;317:865–74.
[19] Gang H, Zhang S. Na^+ permeation and block of hERG potassium channels. J Gen Physiol 2006;128:55–71.

[20] Bahring R, Vardanyan V, Pongs O. Differential modulation of Kv1 channel-mediated currents by co-expression of Kvbeta3 subunit in a mammalian cell-line. Mol Membr Biol 2004;21:19–25.
[21] Tian M, Dong MQ, Chiu SW, Lau CP, Li GR. Effects of the antifungal antibiotic clotrimazole on human cardiac repolarization potassium currents. Br J Pharmacol 2006;147:289–97.
[22] Li GR, Lau CP, Ducharme A, Tardif JC, Nattel S. Transmural action potential and ionic current remodeling in ventricles of failing canine hearts. Am J Physiol 2002;283:H1031–4.
[23] Caballero R, Moreno I, Gonzalez T, Arias C, Valenzuela C, Delpon E, et al. Spironolactone and its main metabolite, canrenoic acid, block human ether-a-go-go-related gene channels. Circulation 2003;107:889–95.
[24] Smith PL, Baukrowitz T, Yellen G. The inward rectification mechanism of the HERG cardiac potassium channel. Nature 1996;379:833–6.
[25] Gao Z, Lau CP, Chiu SW, Li GR. Inhibition of ultra-rapid delayed rectifier K^+ current by verapamil in human atrial myocytes. J Mol Cell Cardiol 2004;36:257–63.
[26] Kamiya K, Mitcheson JS, Yasui K, Kodama I, Sanguinetti MC. Open channel block of HERG K(+) channels by vesnarinone. Mol Pharmacol 2001;60:244–53.
[27] Zhang S, Zhou Z, Gong Q, Makielski JC, January CT. Mechanism of block and identification of the verapamil binding domain to HERG potassium channels. Circ Res 1999;84:989–98.
[28] Yang BF, Xu DH, Xu CQ, Li Z, Du ZM, Wang HZ, et al. Inactivation gating determines drug potency: a common mechanism for drug blockade of HERG channels. Acta Pharmacol Sin 2004;25:554–60.
[29] Su Z, Martin R, Cox BF, Gintant G. Mesoridazine: an open-channel blocker of human ether-a-go-go-related gene K^+ channel. J Mol Cell Cardiol 2004;36:151–60.
[30] Suessbrich H, Schonherr R, Heinemann SH, Lang F, Busch AE. Specific block of cloned Herg channels by clofilium and its tertiary analog LY97241. FEBS Lett 1997;414:435–8.
[31] Watkins CS, Mathie A. Effects on K+ currents in rat cerebellar granule neurones of a membrane-permeable analogue of the calcium chelator BAPTA. Br J Pharmacol 1996;118:1772–8.
[32] Urbano FJ, Buno W. BAPTA-AM blocks both voltage-gated and Ca^{2+}-activated K^+ currents in cultured bovine chromaffin cells. Neuroreport 1998;9:3403–7.
[33] Collatz MB, Rudel R, Brinkmeier H. Intracellular calcium chelator BAPTA protects cells against toxic calcium overload but also alters physiological calcium responses. Cell Calcium 1997;21:453–9.
[34] Dieter P, Fitzke E, Duyster J. BAPTA induces a decrease of intracellular free calcium and a translocation and inactivation of protein kinase C in macrophages. Biol Chem Hoppe Seyler 1993;374:171–4.
[35] Larson L, Arnaudeau S, Gibson B, Li W, Krause R, Hao B, et al. Gelsolin mediates calcium-dependent disassembly of Listeria actin tails. Proc Natl Acad Sci USA 2005;102:1921–6.
[36] Li L, Tucker RW, Hennings H, Yuspa SH. Chelation of intracellular Ca^{2+} inhibits murine keratinocyte differentiation in vitro. J Cell Physiol 1995;163:105–14.
[37] Paschen W, Hotop S, Aufenberg C. Loading neurons with BAPTA-AM activates xbp1 processing indicative of induction of endoplasmic reticulum stress. Cell Calcium 2003;33:83–9.
[38] Pu Y, Chang DC. Cytosolic Ca(2+) signal is involved in regulating UV-induced apoptosis in hela cells. Biochem Biophys Res Commun 2001;282:84–9.
[39] Takahashi K, Inanami O, Kuwabara M. Effects of intracellular calcium chelator BAPTA-AM on radiation-induced apoptosis regulated by activation of SAPK/JNK and caspase-3 in MOLT-4 cells. Int J Radiat Biol 1999;75: 1099–105.
[40] Milnes JT, Crociani O, Arcangeli A, Hancox JC, Witchel HJ. Blockade of HERG potassium currents by fluvoxamine: incomplete attenuation by S6 mutations at F656 or Y652. Br J Pharmacol 2003;139:887–98.
[41] Ridley JM, Milnes JT, Hancox JC, Witchel HJ. Clemastine, a conventional antihistamine, is a high potency inhibitor of the HERG K^+ channel. J Mol Cell Cardiol 2006;40: 107–18.
[42] Ficker E, Jarolimek W, Kiehn J, Baumann A, Brown AM. Molecular determinants of dofetilide block of HERG K^+ channels. Circ Res 1998;82:386–95.
[43] Milnes JT, Witchel HJ, Leaney JL, Leishman DJ, Hancox JC. hERG K^+ channel blockade by the antipsychotic drug thioridazine: an obligatory role for the S6 helix residue F656. Biochem Biophys Res Commun 2006;351: 273–80.
[44] Perry M, Stansfeld PJ, Leaney J, Wood C, de Groot MJ, Leishman D, et al. Drug binding interactions in the inner cavity of HERG channels: molecular insights from structure-activity relationships of clofilium and ibutilide analogs. Mol Pharmacol 2006;69:509–19.
[45] Ridley JM, Milnes JT, Duncan RS, McPate MJ, James AF, Witchel HJ, et al. Inhibition of the HERG K+ channel by the antifungal drug ketoconazole depends on channel gating and involves the S6 residue F656. FEBS Lett 2006;580: 1999–2005.
[46] Sanchez-Chapula JA, Ferrer T, Navarro-Polanco RA, Sanguinetti MC. Voltage-dependent profile of human ether-a-go-go-related gene channel block is influenced by a single residue in the S6 transmembrane domain. Mol Pharmacol 2003;63:1051–8.
[47] Thomas D, Wu K, Wimmer AB, Zitron E, Hammerling BC, Kathofer S, et al. Activation of cardiac human ether-a-go-go related gene potassium currents is regulated by alpha(1A)-adrenoceptors. J Mol Med 2004;82:826–37.
[48] Kiehn J, Karle C, Thomas D, Yao X, Brachmann J, Kubler W. HERG potassium channel activation is shifted by phorbol esters via protein kinase A-dependent pathways. J Biol Chem 1998;273:25285–91.
[49] Thomas D, Zhang W, Wu K, Wimmer AB, Gut B, Wendt-Nordahl G, et al. Regulation of HERG potassium channel activation by protein kinase C independent of direct phosphorylation of the channel protein. Cardiovasc Res 2003;59:14–26.
[50] Chung I, Schlichter LC. Native Kv1.3 channels are upregulated by protein kinase C. J Membr Biol 1997;156: 73–85.
[51] Williams CP, Hu N, Shen W, Mashburn AB, Murray KT. Modulation of the human Kv1.5 channel by protein kinase C activation: role of the Kvbeta1.2 subunit. J Pharmacol Exp Ther 2002;302:545–50.